Journal of Inorganic and General Chemistry
ZAAC
Zeitschrift für anorganische und allgemeine Chemie
DOI: 10.1002/zaac.202000010 SHORT COMMUNICATION

A Terminal Chlorophosphinidene Complex

Josh Abbenseth*[a] and Sven Schneider[a]

Dedicated Prof. Dr. Manfred Scheer on the Occasion of his 65th Birthday

Abstract. Terminal, electrophilic phosphinidene complexes (M=PR) are attractive platforms for PR-transfer to organic substrates. In contrast to aryl- or alkylphosphinidene complexes terminal chlorophosphinidenes (M=PCl) have only been proposed as transient intermediates but isolable example remain elusive. Here we present the transfer of PCl from chloro-substituted dibenzo-7λ^3-phosphanorbornadiene to a square-planar osmium(II) PNP pincer complex to give the first isolable, terminal chlorophosphinidene complex with remarkable thermal stability. Os=P bonding was examined computationally giving rise to highly covalent {Os^{II}=P^{I}Cl} double bonding.

Introduction

While catalytic nitrene transfer has in recent years emerged as powerful tool for C–N formation, efficient phosphinidene (PR) transfer protocols remain scarce.[1] Pioneering work by Niecke and Streubel relied on $SiMe_3Cl$ elimination from chlorotrimethylsilylphosphines and -diphosphines.[2] More recently, strained, bicyclic phosphorus heterocycles, like dibenzo-7λ^3-phosphanorbornadienes that release P–R upon in situ retro Diels–Alder reaction, were heavily exploited as phosphinidene synthons by the Cummins group.[1c,3] In this context, terminal phosphinidene complexes (L_nM=P–R) attracted interest as PR-transfer reagents.[4] For example, stoichiometric phosphirane and phosphirene synthesis has been demonstrated for transient and some isolable electrophilic phosphinidene complexes.[4d,5]

The use of chlorophosphinidene sources could expand the scope of synthetic strategies by P–Cl post-functionalization. *Mathey* and co-workers reported chlorophosphinidene transfer upon thermolysis of a tungsten phosphanorbornadiene complex (Scheme 1).[6] The reaction was proposed to proceed via a transient, terminal chlorophosphinidene intermediate, which evaded characterization presumably owing to high electrophilicity as indicated by DFT computations. *Agapie* and co-workers used chloro-substituted dibenzo-7λ^3-phosphanorbornadiene (ClPA)[3b] for PCl transfer to a molybdenum(0) precursor.[7] However, a terminal Mo^{VI} phosphide complex was obtained upon formal P–Cl oxidative addition (Scheme 1). Importantly, in contrast to aryl- and alkylphosphinidenes, isolable terminal chlorophosphinidene complexes remain elusive.

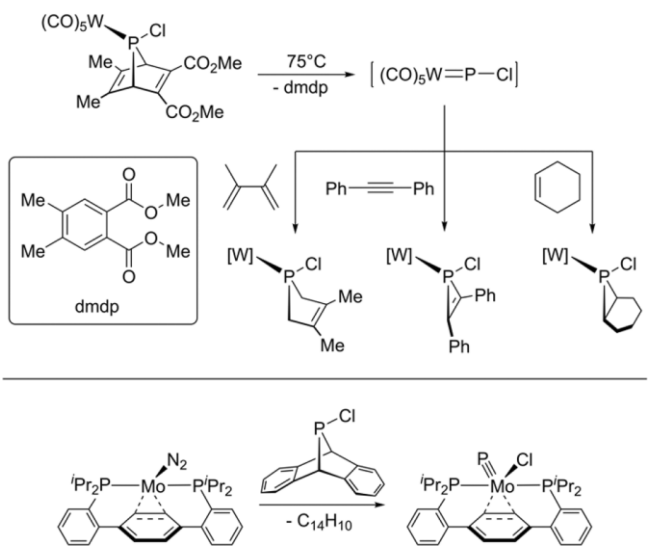

Scheme 1. Proposed formation of a transient chlorophosphinidene complex as phosphinidene transfer reagent reported by *Mathey* and co-workers (top) and molybdenum phosphide synthesis by PCl transfer from *Agapie* and co-workers (bottom).[6,7]

In recent years, our group utilized low-valent and coordinatively unsaturated transition metal pincer platforms to stabilize multiple bonding to group 15 and 16 elements.[8] For this purpose, the square-planar osmium(II) 14-valence-electron species [OsCl(PNP)] (**1**) (PNP = N{CHCHP*t*Bu$_2$}$_2$)[9] proved to be a useful precursor platform.[10] Starting from **1**, we herein report the synthesis and characterization of the first isolable terminal chlorophosphinidene complex.

Results and Discussion

When a freshly prepared solution of **1** is reacted with one equivalent of ClPA at –80 °C in toluene and slowly warmed to

* Dr. J. Abbenseth
E-Mail: josh.abbenseth@chemie.uni-goettingen.de
[a] Universität Göttingen
Institute für Anorganische Chemie
Tammannstraße 4
37077 Göttingen, Germany
Supporting information for this article is available on the WWW under **http://dx.doi.org/10.1002/zaac.202000010** or from the author.

room temperature, a gradual color change from deep purple to reddish-brown is observed (Scheme 2).

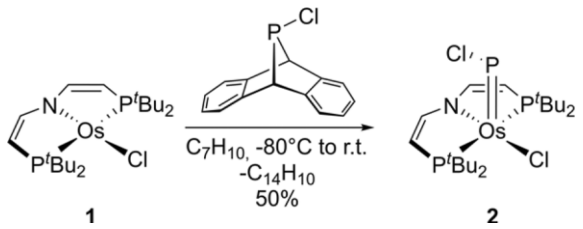

Scheme 2. Synthesis of **2** upon PCl transfer from ClPA to **1**.

$^{31}P\{^1H\}$ NMR spectroscopy reveals selective and quantitative conversion to a new diamagnetic species with signals at $\delta_P = 854.8$ and 70.4 ppm, which are slightly broadened at temperatures between 25 °C and –80 °C. The chemical shifts are consistent with the formation of phosphinidene complex [Os(PCl)Cl(PNP)] (**2**).[11] This value is close to Carty's cationic aminophosphinidene [(η^5-C_5Me_5)Os(PN*i*Pr$_2$)(CO)$_2$][AlCl$_4$] ($\delta(^{31}P)$ = 838 ppm), yet considerably low-field shifted as compared to Lammertsma's osmium arylphosphinidene complexes [(arene)Os(PMes*)L] [$\delta(^{31}P) \approx$ 650–750 ppm; Mes* = 2,4,6-tri-*tert*-butylphenyl; arene = C_6H_6, 1-*i*Pr-4-Me-C_6H_4 (*p*-Cy); L = CO, PPh_3].[12] In comparison, *Tamm* and co-workers reported an NHC-carbene substituted osmium phosphinidenide complex, [(p-Cy)OsCl{P=C(NdippC)$_2$}] (dipp = 2,6-diisopropylphenyl), with partial phosphinidene character and a ^{31}P NMR shift of $\delta(^{31}P)$ = 354 ppm.[13] The ^1H and $^{13}C\{^1H\}$ NMR spectra of complex **2** feature the typical signals of the PNP pincer ligand with overall C_s symmetry on the NMR timescale.

The molecular structure in the solid state confirms the formation of chlorophosphinidene complex **2** (Figure 1). Complex **2** features a distorted square-pyramidal coordination sphere (τ_5 = 0.09)[14] with the phosphinidene ligand in the axial position. The Os–N bond elongates by 0.08 Å with respect to parent **1** as in five-coordinate [Os^{II}Cl(CN*t*Bu)(PNP)] [2.050(3) Å].[9] This is accompanied by a minor Os–Cl bond elongation of 0.03 Å. The Os=P bond length of 2.0699(9) Å is significantly shorter than in Lammertsma's [(*p*-Cy)Os(PMes*)(PPh$_3$)] [*d*(Os=P) = 2.2195(7) Å] and Carty's phosphinidene [(η^5-C_5Me_5)Os(PN*i*Pr$_2$)(CO)$_2$][AlCl$_4$] [*d*(Os=P) = 2.278(2) Å] or in Tamm's phosphinidenide [(*p*-Cy)OsCl{P=C(NdippC)$_2$}] [*d*(Os=P) 2.2230(19) Å], presumably due to the absence of a *trans*-ligand in **2**.[12,13]

The distinct bending of the phosphinidene fragment [Os–P–Cl: 118.64(5)°] is similar to [(*p*-Cy)Os(PMes*)(PPh$_3$)] [Os–P–C: 106.56(9)°] and [(η^5-C_5Me_5)(CO)$_2$Os{PN*i*Pr$_2$}][AlCl$_4$] [Os–P–N: 119.0(2)°], as expected for a 4–electron donating phosphinidene ligand,[15,16] contrasting with only slightly bent Os^{IV} imido complex [Os(NSiMe$_3$)(CN*t*Bu)(PNP)][BPh$_4$] [156.8(3)°].[10a] The P–Cl bond of **2** [2.1759(12) Å] is notably longer than the computed value for [W(PCl)(CO)$_5$] [*d*(P–Cl)^{DFT} = 2.107 Å].[6]

The computed frontier molecular orbital diagram of **2** (Figure 2) features a lowest unoccupied molecular orbital (LUMO) with distinct Os–P π–antibonding character and high

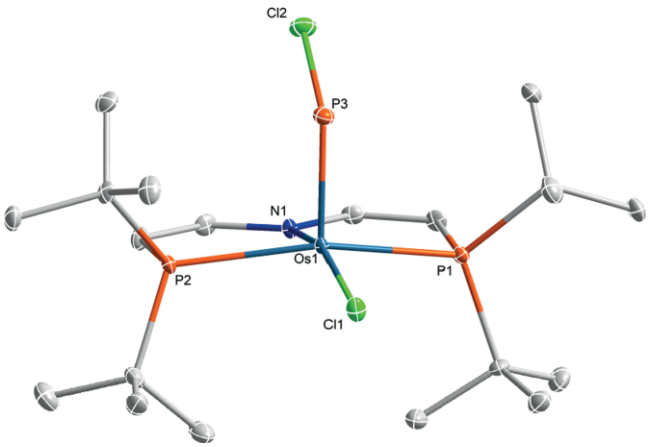

Figure 1. Molecular structure of complex **2** from single-crystal X-ray diffraction (thermal ellipsoids drawn at 50% probability level); hydrogen atoms are omitted for clarity. Selected bond lengths /Å and angles /°: Os1–Cl1 2.3873(8), Os1–N1 2.056(3), Os1–P1 2.3942(9), Os1–P2 2.4073(9), Os1–P3 2.0699(9) P3–Cl2 2.1759(12), N1–Os1–Cl1 162.46(8), P1–Os1–P2 157.34(3), N1–Os1–P3 93.69(8), Os1–P3–Cl2 118.64(5).

phosphorus contribution. The highest occupied molecular orbital (HOMO) is mainly located on the unsaturated pincer ligand, reminiscent of the silylimide [Os(NTMS)(CN*t*Bu)(PNP)][BPh$_4$].[10a] The computed Wiberg (1.58) and Mayer (1.99) bond orders for the osmium-phosphinidene bond support double bond character, which is increased with respect to the phosphinidenide complex [(*p*-Cy)OsCl{P=C(NdippC)$_2$}] (WBI_{OsP} = 1.49).[13]

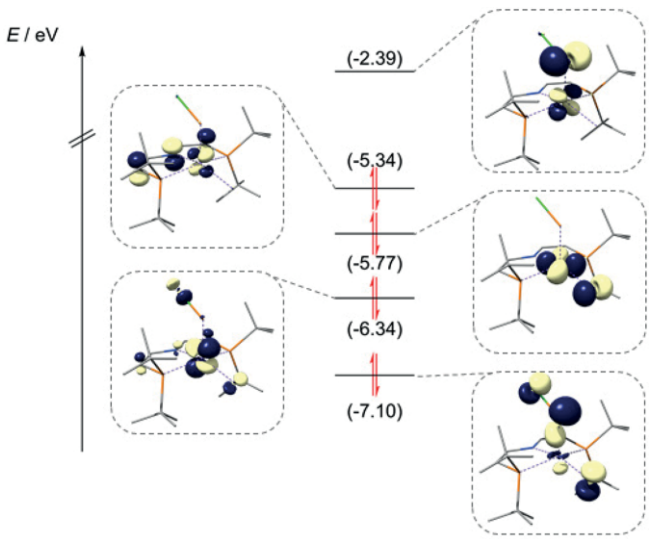

Figure 2. Computed molecular orbital diagram of **2** (D3BJ-PBE0-RIJCOSX/def2-TZVP//D3BJ-PBE-RI/def2-SVP); energies are given in eV.

Within the natural localized molecular orbital (NLMO) description, complex **2** features two predominantly non-bonding, Os-based NLMOs (Figure 3, top). A P-centered orbital with high s-character (sp$^{0.2}$) represents the stereochemically active lone pair at phosphorus. P–Os σ–bonding is highly covalent (54% Os, 44% P), as was similarly found for [(η^5-C_5Me_5)

$Os(PN^iPr_2)(CO)_2]^+$,[16] while the π bond is slightly more polarized towards the metal (67 % Os, 28 % P), supporting polar covalent Os=P double bonding. In analogy to Fischer-type carbenes,[12b] **2** is best described by the $(PNP)Os^{II}=P^{I}Cl$ representation with small charge transfer upon recombination despite both free fragments adopting triplet ground states.[9,17]

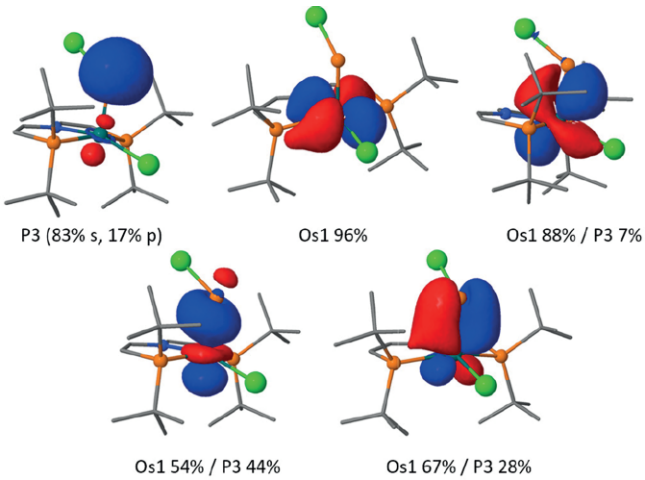

Figure 3. Computed NLMOs of **2** with their respective orbital or element compositions; contributions under 1 % are neglected (D3BJ-PBE0-RIJCOSX/def2-TZVP//D3BJ-PBE-RI/def2-SVP [NBO 6.0]).

The DFT computations further reveal that the PCl moiety can rotate on a relatively flat potential energy surface ($\Delta G^{\ddagger}_{DFT}$ = 9.81 kcal·mol^{-1}, ΔG_{DFT} = 5.03 kcal·mol^{-1}), in line with broadened signals in the ^{31}P NMR spectrum. Furthermore, P–Cl oxidative addition, as reported by Agapie,[7] was evaluated. The osmium(VI) phosphide $[Os(P)Cl_2(PNP)]$ (**3**) was computed considerably higher in free energy than **2** by ΔG_{DFT} = 34.3 kcal·mol^{-1} and therefore not accessible at room temperature.[11] In fact, **2** exhibits surprising thermal stability evenupon heating to 80 °C in benzene over several hours. Furthermore, no reaction was observed with equimolar amounts of cyclohexadiene, tolane or 2,3-dimethylbutadieneat elevated temperatures (80 °C in benzene) over the course of multiple hours. Despite the low-lying, P-centered LUMO of **2**, PCl-transfer is probably impeded by the bulky *t*Bu substituents that shield the phosphinidene moiety from nucleophilic attack.

Conclusions

In summary, the synthesis the first isolable chlorophosphinidene complex is reported upon PCl transfer from ClPA to a coordinatively unsaturated osmium(II) complex. The $Os^{II}=P^{I}Cl$ double bond shows a high degree of covalency with slight polarization towards the metal. The computations further indicate a phosphorus centered, low-lying LUMO. However, high thermal and chemical stability with respect to phosphinidene transfer is attributed to efficient steric shielding induced by the bulky *t*Bu groups of the pincer ligand.

Experimental Section

Materials and Methods: All experiments were carried out using standard glovebox (argon atmosphere) techniques. Solvents were dried by passing through columns packed with activated alumina. CD_2Cl_2 (Eurisotop GmbH) was dried with CaH_2 distilled by trap-to-trap transfer in vacuo and degassed by three freeze-pump-thaw cycles. Activated charcoal was heated under high-vacuum for 3 d at 150 °C prior to use. Complex ClPA and **1** were prepared according to previously reported procedures.[3b,9] Elemental analysis was obtained from the analytical laboratories at the Georg-August University. NMR spectra were recorded on a Bruker Avance III HD 400 spectrometer and calibrated to the residual solvent proton resonance (CD_2Cl_2 δ_H = 5.32 ppm). LIFDI mass spectrometry was performed on a Jeol AccuTOF spectrometer under inert conditions.

Synthesis of 2: A freshly prepared solution of **1** (15 mg, 25.8 µmol, 1.0 equiv.) in toluene (0.5 mL) was cooled to –80 °C, an equimolar amount of ClPA was added and the solution was warmed to room temperature over the course of 1 h under intense stirring. After filtration, the solvent was removed. DCM (1 mL) was added and the solution was cooled to –80 °C for 4 h. The precipitated anthracene was decanted off and more anthracene crystallized from DCM/pentane (0.5 mL / 5 mL) at –80 °C. The anthracene was again decanted off and the obtained solution was subjected to an activated charcoal column (3 × 0.5 cm). The solvent was removed, the crude product was layered with pentane (3 mL), and stored at –30 °C for 2 d. The solution was decanted and the solid was dissolved in a minimal amount of benzene (0.3 mL) and lyophilized. **2** (8.5 mg, 13.1 µmol, 50 %) was obtained as a purple solid. $C_{20}H_{40}Cl_2NOsP_3$ (648.6): calcd. C, 37.0; H, 6.22; N, 2.16 %; found: C, 37.4; H, 6.53; N, 2.03 %. Even after prolonged drying in vacuo (2 d) a small amount of benzene was observed in the NMR spectra. **NMR** (CD_2Cl_2, RT): ^{1}H NMR (400 MHz): δ = 7.36 (A_9BCXX'A'$_9$B'C', $N = |^3J_{CX}+{}^4J_{CX'}|$ = 35.7, $^3J_{BC}$ = 6.1 Hz, 2 H, NC*H*), 4.32 (A_9BCXX'A'$_9$B'C', $N = |^2J_{BX}+{}^4J_{BX'}|$ = 6.6, $^3J_{BC}$ = 6.1 Hz, 2 H, PC*H*), 1.37 [A_9BCXX'A'$_9$B'C', $^3J_{AX}$ = 14.7 Hz, 18 H, P(C(CH_3)$_3$)], 14.3 [A_9BCXX'A'$_9$B'C', $^3J_{AX}$ = 14.3 Hz, 18 H, P(C(CH_3)$_3$)]. ^{13}C{^{1}H} NMR (128.8 MHz): δ = 168.1 (vt, $N = |^2J_{CP} + {}^3J_{CP}|$ = 5.6 Hz, 2C, N*C*H), 87.2 (vt, $N = |^1J_{CP} + {}^3J_{CP}|$ = 23.4 Hz, 2C, P*C*H), 40.1 [vt, $N = |^1J_{CP} + {}^2J_{CP}|$ = 12.5 Hz, 2C, P(*C*(CH_3))], 35.9 [vt, $N = |^1J_{CP} + {}^2J_{CP}|$ = 11.0 Hz, 2C, P(*C*(CH_3))], 29.8 [vt, $N = |^2J_{CP} + {}^4J_{CP}|$ = 2.3 Hz, 6C, P(C(*C*H$_3$)$_3$)], 29.4 [br, 6C, P(C(*C*H$_3$)$_3$)]. ^{31}P{^{1}H} NMR (202.5 MHz): δ = 858.4 (s br, 1P, *P*Cl), 70.4 [s br, 2P, *P*(C(CH_3)$_3$)]. **LIDFI-MS** (toluene): 649.2 ([M$^+$]).

Crystallographic Details: Single crystals for X-ray structure determination were mounted in protective perfluoro polyether oil in a cold N_2 stream on the diffractometer. Diffraction data were obtained at 100 K on a Bruker D8 three-circle diffractometer, equipped with a PHOTON 100 CMOS detector and an INCOATEC microfocus source with Quazar mirror optics (Mo-K_α radiation, λ = 0.71073 Å). The data were integrated with SAINT and a semi-empirical absorption correction from equivalents with SADABS was applied. The structure was solved and refined using the Bruker SHELX 2014 software package.[18] Non-hydrogen atoms were refined with anisotropic displacement parameters and hydrogen atoms isotropically on calculated positions using a riding model.

Crystallographic data (excluding structure factors) for the structure in this paper have been deposited with the Cambridge Crystallographic Data Centre, CCDC, 12 Union Road, Cambridge CB21EZ, UK. Copies of the data can be obtained free of charge on quoting the depository number CCDC-1976007 (for **2**) (Fax: +44-1223-336-033; E-Mail: deposit@ccdc.cam.ac.uk, http://www.ccdc.cam.ac.uk)

Computational Details: DFT calculations were carried out with the ORCA 4.0.1.2[19] program package using the PBE[20] and PBE0[21]

functionals, respectively. Ahlrichs' basis sets def2-SVP (for geometry optimization and frequency calculation) and def2-TZVP (for single-point energies) were used with a full basis for all elements but Os for which the Stuttgart-Dresden 60 electron core potential was chosen to replace the inner shell 1s-4f orbitals.,[22,23] The RI-J[24] (PBE) and RIJCOSX (PBE0) approximations in combination with the corresponding auxiliary basis sets were utilized to reduce computational costs in the geometry optimizations, frequency calculations and single point calculations. Grimme's model (D3) with Becke-Johnson damping[25] was used to account for dispersion with the PBE or PBE0 functionals. No symmetry restrains were imposed and the optimized structures were defined as minima (no negative eigenvalues) or transitions states (one negative eigenvalue) by vibrational analyses. NLMO analysis of **2** was carried out with NBO 6.0 and visualized with jmol.[26,27] Geometries were analyzed and visualized with Cylview[28] and molecular orbitals were visualized with Chimera.[29]

Supporting Information (see footnote on the first page of this article): Spectroscopic and crystallographic details of **2**.Coordinates of all computed species and their respective energies.

Acknowledgements

The authors thank the European Research Council (ERC Grant Agreement 646747 to S.Sch.) and the Fond der Chemischen Industrie (FCI Stipendium for J.A.) for financial support. Open access funding enabled and organized by Projekt DEAL.

Keywords: Phosphinidene; Osmium; Pincer; Density functional calculations; Natural localized molecular orbital (NLMO)

References

[1] a) K. Pal, O. B. Hemming, B. M. Day, T. Pugh, D. J. Evans, R. A. Layfield, *Angew. Chem. Int. Ed.* **2016**, *55*, 1690; b) J. K. Pagano, B. J. Ackley, R. Waterman, *Chem. Eur. J.* **2018**, *24*, 2554; c) M. B. Geeson, W. J. Transue, C. C. Cummins, *J. Am. Chem. Soc.* **2019**, *141*, 13336.

[2] a) E. Niecke, R. Streubel, M. Nieger, D. Stalke, *Angew. Chem. Int. Ed. Engl.* **1989**, *28*, 1673; b) R. Streubel, E. Niecke, *Chem. Ber.* **1990**, *123*, 1245; c) R. Streubel, E. Niecke, P. Paetzold, *Chem. Ber.* **1991**, *124*, 765; d) E. Niecke, R. Streubel, M. Nieger, *Angew. Chem. Int. Ed. Engl.* **1991**, *30*, 90.

[3] a) A. Velian, C. C. Cummins, *J. Am. Chem. Soc.* **2012**, *134*, 13978; b) A. Velian, M. Nava, M. Temprado, Y. Zhou, R. W. Field, C. C. Cummins, *J. Am. Chem. Soc.* **2014**, *136*, 13586; c) W. Transue, A. Velian, M. Nava, C. García-Iriepa, M. Temprado, C. C. Cummins, *J. Am. Chem. Soc.* **2017**, *139*, 10822; d) K. M. Szkop, M. B. Geeson, D. W. Stephan, C. C. Cummins, *Chem. Sci.* **2019**, *10*, 3627; e) M. B. Geeson, W. J. Transue, C. C. Cummins, *J. Am. Chem. Soc.* **2019**, *141*, 13336.

[4] a) R. J. Gilliard, J. M. Kieser, J. D. Protasiewicz, *Synthons for the Development of New Organophosphorus Functional Materials in Main Group Strategies towards Functional Hybrid Materials* (Eds T. Baumgartner, F. Jäkle) **2018**; b) L. Dostál, *Coord. Chem. Rev.* **2017**, *353*, 142; c) J. C. Slootweg, K. Lammertsma, *Sci. Synth.* **2009**, *42*, 15; d) F. Mathey, *Dalton Trans.* **2007**, 1861; e) R. Waterman, *Dalton Trans.* **2009**, 18; f) K. Lammertsma, M. J. M. Vlaar, *Eur. J. Org. Chem.* **2002**, 1127.

[5] a) A. L. Colebatch, B. J. Frogles, A. F. Hill, *Dalton Trans.* **2019**; *48*, 10628; b) P. Mathur, S. Misra, *Adv. Organomet. Chem.* **2019**, DOI.org/10.1016/bs.adomc.2019.09.001.

[6] M. P. Duffy, F. Mathey, *J. Am. Chem. Soc.* **2009**, *131*, 7534.

[7] J. A. Buss, P. H. Oyala, T. Agapie, *Angew. Chem. Int. Ed.* **2017**, *56*, 14502.

[8] a) B. Askevold, J. Torres Nieto, S. Tussupbayev, M. Diefenbach, E. Herdtweck, M. C. Holthausen, S. Schneider, *Nature Chem.* **2011**, *3*, 532; b) M. G. Scheibel, B. Askevold, F. Heinemann, E. I. Reijerse, B. de Bruin, S. Schneider, *Nature Chem.* **2012**, *4*, 552; c) M. G. Scheibel, Y. Wu, A. C. Stückl, L. Krause, E. Carl, D. Stalke, B. de Bruin, S. Schneider, *J. Am. Chem. Soc.* **2013**, *135*, 17719; d) J. Abbenseth, M. Finger, C. Würtele, M. Kasanmascheff, S. Schneider, *Inorg. Chem. Front.* **2016**, *3*, 469; e) F. S. Schendzielorz, M. Finger, C. Volkmann, C. Würtele, S. Schneider, *Angew. Chem. Int. Ed.* **2016**, *55*, 11417; f) M. Kinauer, M. Diefenbach, H. Bamberger, S. Demeshko, E. J. Reijerse, C. Volkmann, C. Würtele, J. van Slageren, B. de Bruin, M. C. Holthausen, S. Schneider, *Chem. Sci.* **2018**, *9*, 4325; g) D. Delony, M. Kinauer, M. Diefenbach, S. Demeshko, C. Würtele, M. C. Holthausen, S. Schneider, *Angew. Chem. Int. Ed.* **2019**, *58*, 10966; h) J. Abbenseth, M. Diefenbach, A. Hinz, L. Alig, C. Würtele, J. M. Goicoechea, M. Holthausen, S. Schneider, *Angew. Chem. Int. Ed.* **2019**, *58*, 10971.

[9] J. Abbenseth, M. Diefenbach, S. C. Bete, C. Würtele, C. Volkmann, S. Demeshko, M. C. Holthausen, S. Schneider, *Chem. Commun.* **2017**, *53*, 5511.

[10] a) J. Abbenseth, S. C. Bete, M. Finger, C. Volkmann, C. Würtele, S. Schneider, *Organometallics* **2018**, *37*, 802; b) J. Abbenseth, D. Delony, M. C. Neben, C. Würtele, B. de Bruin, S. Schneider, *Angew. Chem. Int. Ed.* **2019**, *58*, 6338.

[11] See the Supporting Information for spectroscopic, crystallographic, and computational details.

[12] a) A. T. Termaten, T. Nijbacker, M. Schakel, M. Lutz, A. L. Spek, K. Lammertsma, *Chem. Eur. J.* **2003**, *9*, 2200; b) B. T. Sterenberg, K. A. Udachin, A. J. Carty, *Organometallics* **2003**, *22*, 3927.

[13] M. Peters, A. Doddi, T. Bannenberg, M. Freytag, P. G. Jones, M. Tamm, *Inorg. Chem.* **2017**, *56*, 10785.

[14] A. W. Addison, T. N. Rao, J. Reedijk, J. van Rijn, G. C. Verschoor, *J. Chem. Soc., Dalton Trans.* **1984**, 1349.

[15] K. Lammertsma, *Top. Curr. Chem.* **2003**, *229*, 95.

[16] K. K. Pandey, P. Tiwari, P. Patidar, *J. Phys. Chem. A* **2012**, *116*, 11753.

[17] a) K. P. Huber, G. Herzberg, *Molecular Spectra and Molecular Structure of Diatomic Molecules*, Van Nostrand, New York, **1979**; b) E. Rincón, P. Pérez, E. Chamorro, *Chem. Phys. Lett.* **2007**, *448*, 273.

[18] a) APEX3 v2016.9–0 (SAINT/SADABS/SHELXT/SHELXL), Bruker AXS Inc., Madison, WI, USA, **2016**; b) G. M. Sheldrick, *Acta Crystallogr., Sect. A* **2015**, *71*, 3; c) G. M. Sheldrick, *Acta Crystallogr., Sect. A* **2015**, *71*, 3; d) G. M. Sheldrick, *Acta Crystallogr., Sect. A* **2008**, *64*, 112.

[19] F. Neese, *WIREs Comput. Mol. Sci.* **2012**, *2*, 73.

[20] J. P. Perdew, K. Burke, M. Ernzerhof, *Phys. Rev. Lett.* **1996**, *77*, 3865.

[21] J. P. Perdew, K. Burke, M. Ernzerhof, *J. Chem. Phys.* **1996**, *105*, 9982.

[22] F. Weigend, R. Ahlrichs, *Phys. Chem. Chem. Phys.* **2005**, *7*, 3297.

[23] D. Andrae, U. Häussermann, M. Dolg, H. Stoll, H. Preuss, *Theor. Chim. Acta* **1990**, *77*, 123.

[24] a) O. Treutler, R. Ahlrichs, *J. Chem. Phys.* **1995**, *102*, 346; b) O. Treutler, R. Ahlrichs, *Chem. Phys. Lett.* **1995**, *240*, 283; c) O. Treutler, R. Ahlrichs, *Chem. Phys. Lett.* **1995**, *242*, 652; d) K. Eichkorn, F. Weigend, O. Treutler, R. Ahlrichs, *Theo. Chem. Acc.* **1997**, *97*, 119.

[25] a) S. Grimme, S. Ehrlich, L. Goerigk, *J. Comput. Chem.* **2011**, *32*, 1456; b) S. Grimme, J. Antony, S. Ehrlich, H. Krieg, *J. Chem. Phys.* **2010**, *132*, 154104.

[26] NBO 6.0. E. D. Glendening, J. K. Badenhoop, A. E. Reed, J. E. Carpenter, J. A. Bohmann, C. M. Morales, C. R. Landis, F. Wein-

hold, Theoretical Chemistry Institute, University of Wisconsin, Madison **2013**.
[27] Jmol: An open-source Java viewer for chemical structures in 3D. http://www.jmol.org/.
[28] C. Y. Legault, CYLview (http://www.cylview.org).
[29] E. F. Pettersen, T. D. Goddard, C. C. Huang, G. S. Couch, D. M. Greenblatt, E. C. Meng, T. E. Ferrin, *J. Comput. Chem.* **2004**, *25*, 1605.

Received: January 8, 2020
Published Online: February 11, 2020

